

# Self-assembly of ionic surfactants and formation of mesostructures

Aniket Bhattacharya<sup>1,2,3</sup> and S D Mahanti<sup>1</sup>

<sup>1</sup> Department of Physics and Astronomy, Michigan State University, East Lansing, MI 48824-1116, USA

<sup>2</sup> Department of Physics, University of Central Florida, Orlando, FL 32816-2385, USA

E-mail: aniket@physics.ucf.edu

Received 24 July 2000, in final form 8 December 2000

## Abstract

Self-assembly of ionic surfactants resulting in micelle formation is studied using off-lattice Monte Carlo simulation in two dimensions (2D). We find that in addition to the Lennard-Jones (LJ) interaction, which acts among all of the particles, a screened Coulomb interaction, acting only among the surfactant heads, makes the geometric arrangement of micelles very different compared to that for neutral surfactants at the same density. At low concentrations, ionic surfactants produce spherical micelles and exhibit intermicellar ordering arising out of the longer-range repulsion of the surfactant head groups. For larger concentrations, they tend to form bi-layers. Motivated by recent experiments on preparation of mesoporous sieves through surfactant-templating routes, we then extend these studies to micellization of ionic surfactants in the presence of other neutral host particles. The morphologies of the surfactant–host composites are studied as functions of host particle densities, sizes, and their interaction strengths. Assuming the presence of micelles as quenched disorder, we obtain a qualitative understanding of the local ordering of the host particles in terms of a dimensionless density parameter from the known liquid–vapour phase diagram in 2D of a LJ fluid.

## 1. Introduction

Synthesis of nanophases and mesophases of matter [1–5] by exploiting the self-assembling properties of neutral and ionic surfactants [6, 7] has recently been realized to be an extremely efficient method since the size and shape can be predictively controlled by adjustment of the surfactant chain lengths and concentrations. Mesoporous sieves of pore diameters up to a few 100 Å have been synthesized using surfactants as structure-directing elements. More recently the same technique has been extended to prepare mesoporous structures at the air–water [8]

<sup>3</sup> Author to whom any correspondence should be addressed. Permanent address: Department of Physics, University of Central Florida, Orlando, FL 32816-2385, USA.

and oil–water interfaces [9] as well. From a technological point of view, the underlying ideas of such syntheses have been appreciated by the broad scientific community because the general procedure resembles naturally occurring biomineralization where an organic structure-directing seed dictates further growth of inorganic materials [10]. Progress in synthesis via surfactant-directed templating has brought out new ideas which go beyond the standard *biomimetic* approaches.

In a typical synthesis process, surfactants in solution form micelles of various shapes [7, 11]. Addition of inorganic host particles may strongly affect the phase diagram of surfactant aggregation [12]. Therefore, instead of starting with a pre-organized organic surfactant template, one may think of an alternative route where the surfactant self-assembly gets modified by the presence of these inorganic host particles. This alternative approach of *cooperative self-assembly* [2, 3] is not only technologically more versatile, but the process of self-organization is theoretically very appealing as well. The solvent–surfactant–host system is reminiscent of oil–water–surfactant ternary systems [13]. A variety of structures, e.g., liquid-crystalline structures of different symmetry [1] and bi-continuous structures [5], are naturally possible for these systems; some of these have already been observed experimentally. While all of these surfactant-templating routes lead to porous media of large internal diameter, structurally the media can be very different. For example, cylindrical mesotubes which are synthesized with the use of ionic surfactants exhibit lateral hexagonal ordering [1], whereas those which are synthesized using neutral surfactants [4] form worm-hole-like structures lacking such periodicity. The aim of this paper is to study self-assembly of these surfactant–host composite structures using a simple model of a surfactant–host system involving Lennard-Jones (LJ), screened Coulomb (SC), and bond-bending potentials.

In a previous paper [14] (hereafter to be referred to as **I**) we have described the results of an extensive study of the self-assembly of neutral surfactants using an off-lattice Monte Carlo (MC) scheme. We also reported briefly some results for ionic surfactants interacting through a screened Coulomb repulsion. A special feature of our model, used in this paper and **I**, is that the solvent particles are not explicitly present in the model. The effect of the solvent particles (water) which introduce hydrophilic and hydrophobic forces are implicit in the effective interaction parameters for the surfactants. Similar methods have been adopted in simulation studies of aggregation properties of short block-copolymers [15, 16]. In addition, for the ionic surfactants the effect of water is to act as a dielectric and screen the bare Coulomb repulsion. Since the solvent particles do not enter into the computational scheme explicitly, the model has been found to be extremely efficient for studying multimicellar systems. In **I**, where we studied micellar aggregation of neutral surfactants in considerable detail, an ensemble averaging over many different initial configurations for reasonably large system sizes was feasible because of this efficient scheme. A detailed comparison of our results with previous numerical work [17–23] (where solvent degrees of freedom were taken into account explicitly) showed that our model produced a qualitatively similar picture of micelle formation [14].

In the first part of this paper we study in detail the aggregation properties of model ionic surfactants to find out to what extent our model captures the general properties of ionic micelles. In fact, we find that this simple model can describe the essential characteristics of ionic micelles. In the second half, we use the same model to study the surfactant-induced ordering and morphologies of the other host particles mentioned before. In the same spirit as in **I**, we have considered here a 2D system. Because of this restriction and other simplifications, nowhere have we tried to be quantitative in comparing our simulation results with actual experiments. But we show that our results contain important qualitative information which is of general interest and may be relevant as regards promoting further experiments. In the following section we describe the model briefly. A more detailed discussion of the model with

references to previous work can be found in **I**. We then present our simulation results for the ionic surfactants. From these studies we choose a suitable set of parameters and study the effect of the incorporating host particles on micelle formation. Finally, we discuss possible connections of these simulation results to experiments and suggest further refinements of the model.

## 2. Model

We consider a 2D continuum model in which each surfactant is represented by a chain consisting of  $N_m$  monomers connected by rigid bonds. The first monomer is considered to be the head ( $h$ ) and the remaining  $N_m - 1$  monomers represent the tail particles ( $t$ ). There are altogether  $N_c$  surfactants and the total potential energy is written as

$$U = \sum_{i < j} \phi_{ij}^{LJ}(r_{ij}) + \sum_{i'} U_{i'}^b + \sum_{\mu < \nu} U_{\mu\nu}^{sc}(r_{\mu\nu}). \quad (1)$$

The first term introduces an LJ-type pairwise potential between any two monomers (to mimic the hydrophobic and hydrophilic interactions between surfactants), and is of the form

$$\phi_{ij}^{LJ}(r_{ij}) = \begin{cases} 4\epsilon_{ij} \left[ \left( \frac{\sigma_{ij}}{r_{ij}} \right)^{12} - \left( \frac{\sigma_{ij}}{r_{ij}} \right)^6 \right] - \phi_0(R_{ij}^c) & r_{ij} < R_{ij}^c \\ 0 & r_{ij} \geq R_{ij}^c \end{cases} \quad (2)$$

where  $r_{ij} = |\vec{r}_i - \vec{r}_j|$ , and  $\epsilon_{ij}$ ,  $\sigma_{ij}$ , and  $R_{ij}^c$  are the LJ parameters and cut-off distances for the pair of monomers  $i$  and  $j$  respectively. The term

$$\phi_0(R_{ij}^c) = 4\epsilon_{ij} \left[ \left( \frac{\sigma_{ij}}{R_{ij}^c} \right)^{12} - \left( \frac{\sigma_{ij}}{R_{ij}^c} \right)^6 \right]$$

causes the potential to go continuously to zero at the cut-off distance  $R_{ij}^c$ .

The second term incorporates the bond-bending potential between any two successive bonds and is given by

$$U_{i'}^b = R_b(\theta_{i'} - \theta_0)^2 \quad (3)$$

where  $i'$  represents any monomer except the first one and the last one in a given chain. The angle  $\theta_{i'}$  subtended by two successive bonds on either side of the monomer  $i'$  is expressed as

$$\theta_{i'} = \cos^{-1} \frac{(\vec{r}_{i'-1} - \vec{r}_{i'}) \cdot (\vec{r}_{i'} - \vec{r}_{i'+1})}{|\vec{r}_{i'-1} - \vec{r}_{i'}| \cdot |\vec{r}_{i'} - \vec{r}_{i'+1}|}. \quad (4)$$

In equation (3),  $\theta_0$  is the equilibrium value of  $\theta_i$ . In our calculations we have chosen  $\theta_0 = \pi$  but treat  $R_b$  as a parameter.

For ionic surfactants containing charged head groups we introduce a SC repulsion between two head units. This model needs some justification. When one has charged surfactants in a solvent there is an equal concentration of counter-charges in the solvent. For example, for the commonly used surfactant cetyl-trimethyl-ammonium (CTA<sup>+</sup>), the counter-ion can be Cl<sup>-</sup> or Br<sup>-</sup>. Thus one has a soup of very heavy surfactants (atomic weight >150 amu), light water particles (atomic weight 18 amu), and medium-weight halogen ions (atomic weight roughly 37 amu or 70 amu). Thus to a good approximation one can treat the lighter particles as moving and screening the bare Coulomb repulsion between charged but heavy surfactants. This is physically quite similar to the role of electrons (light mass) in screening the bare Coulomb interaction between heavy ions in solids. The next step is to explicitly incorporate the heavy

surfactants and the medium-weight halogen counter-ions. In this paper we treat the counter-ions as a part of the screening medium for simplicity. For the screened Coulomb repulsion we use the standard Debye–Huckel (D–H) form [11]

$$U_{\mu\nu}^{sc}(r_{\mu\nu}) = u_0 \frac{\exp(-\kappa r_{\mu\nu})}{r_{\mu\nu}} \quad (5)$$

where the indices  $\mu$  and  $\nu$  run over the surfactant heads only. The interaction strength  $\kappa^{-1}$  is the D–H screening length and  $u_0$  is a function of the total charge of a surfactant. We will use  $u_0$  and  $\kappa$  as phenomenological parameters<sup>4</sup>. A cut-off distance  $R_{ij}^{SC}$  is introduced such that  $U_{\mu\nu}^{sc}(R_{\mu\nu}^{SC}) \sim \phi_0(2.5\sigma_{tt})$ . This gives  $R_{ij}^{SC} \sim 30\sigma_{tt}$ . The amphiphilic characteristics of the surfactants are introduced through the choice of two different cut-off distances for the LJ interaction [14]. For any two particles  $i$  and  $j$ , a cut-off distance  $R_{ij}^c = 2^{1/6}\sigma_{ij}$  introduces a purely repulsive interaction, whereas a choice of  $R_{ij}^c = 2.5\sigma_{ij}$  introduces an attractive LJ tail. We consider surfactants with hydrophilic heads and hydrophobic tails which are modelled with the appropriate cut-off parameters  $R_{hh}^c = 2^{1/6}\sigma_{hh}$ ,  $R_{ht}^c = 2^{1/6}\sigma_{ht}$ , and  $R_{tt}^c = 2.5\sigma_{tt}$ .

Finally, the host particles ( $p$ ) are represented as simple monomers interacting among themselves and with the surfactants through a LJ potential. For simplicity, we have considered particles with an attractive LJ interaction among themselves. We introduce a repulsive tail–particle and an attractive head–particle interaction in order that the host particles preferentially lie outside the core of the micelles. The units of length and the temperature ( $T$ ) have been chosen as  $\sigma_{tt}$  and  $\epsilon_{tt}/k_B$  respectively. With the introduction of LJ interactions among the particles and the surfactants, the indices  $i$  and  $j$  in  $\epsilon_{ij}$  and  $\sigma_{ij}$  can refer to either a head ( $h$ ), a tail ( $t$ ), or a host particle ( $p$ ). Since  $\epsilon_{ij}$  and  $\sigma_{ij}$  are symmetric in  $i$  and  $j$ , they can in general take any of six independent values. For our simulation we have chosen  $\sigma_{hh}/\sigma_{tt} = 2$  so that the ionic heads are bigger than the tail particles.  $\sigma_{pp}/\sigma_{tt}$  lies between  $\sim 1$  and 2. The off-diagonal  $\sigma_{ij}$  ( $i \neq j$ ) are not chosen independently. They are obtained from the diagonal elements as  $\sigma_{ij} = (\sigma_{ii} + \sigma_{jj})/2$ . All of the  $\epsilon_{ij}$  (in units of  $\epsilon_{tt}$ ) are chosen to be unity except  $\epsilon_{pp}$  and  $\epsilon_{hp}$ . We carry out simulations for different ratios  $\epsilon_{pp}/\epsilon_{hp}$ . The bond lengths  $l_{i,j}$  between any two successive monomers of a given surfactant are chosen to be equal to the corresponding  $\sigma_{ij}$ . The simulations are done at  $T = 0.5$ . The values of the interaction parameters, including the cut-off distances, are summarized in table 1.

**Table 1.**

$\sigma_{hh}/\sigma_{tt}$	$\sigma_{ht}/\sigma_{tt}$	$\sigma_{pp}/\sigma_{tt}$	$\sigma_{hp}/\sigma_{tt}$	$\sigma_{pt}/\sigma_{tt}$	
2.0	$\frac{1}{2}(\sigma_{hh}/\sigma_{tt} + 1)$	1.0, 2.0	$\frac{1}{2}(\sigma_{hh}/\sigma_{tt} + \sigma_{pp}/\sigma_{tt})$	$\frac{1}{2}(\sigma_{pp}/\sigma_{tt} + 1)$	
$\epsilon_{hh}/\epsilon_{tt}$	$\epsilon_{ht}/\epsilon_{tt}$	$\epsilon_{pp}/\epsilon_{tt}$	$\epsilon_{hp}/\epsilon_{tt}$	$\epsilon_{pt}/\epsilon_{tt}$	
2.0	1.0	0.5, 1.0	0.5, 1.0	1.0	
$R_{hh}/\sigma_{hh}$	$R_{ht}/\sigma_{ht}$	$R_{pp}/\sigma_{pp}$	$R_{hp}/\sigma_{hp}$	$R_{pt}/\sigma_{pt}$	$R_{tt}/\sigma_{tt}$
$2^{1/6}$	$2^{1/6}$	2.5	2.5	$2^{1/6}$	2.5

The Monte Carlo moves consist of off-lattice counterparts of forward and backward *slithering-snake* reptation moves [24] of the surfactants, and *kink-jumps* [25] of the individual monomers as described in detail in I. In this work, we have introduced a *generalized kink-jump algorithm* for those particles with *unequal bond lengths on either side* as described below. The

<sup>4</sup> A typical value of  $\kappa \simeq 0.1$ , which corresponds to a distance  $\sim 10\sigma_{tt}$ . This is approximately the average intermicellar distance. Since micelles are uniformly distributed, this serves as a *a posteriori* justification for treating the SC interaction as isotropic.

usual kink-jump is the off-lattice counterpart of the Verdier–Stockmayer model [25] which consists of putting the inner  $i$ th particle into its mirror image position along the bond joining its adjacent monomers, satisfying the following equation:

$$\vec{R}'_i = \vec{R}_{i+1} + \vec{R}_{i-1} - \vec{R}_i \quad (6)$$

and the end particles are then rotated according to

$$\begin{aligned} \vec{R}'_1 &= \vec{R}_2 + \vec{\psi}_1 \\ \vec{R}'_{N_m} &= \vec{R}_{N_m} + \vec{\psi}_m \end{aligned} \quad (7)$$

where  $\vec{\psi}_1$  and  $\vec{\psi}_m$  are two randomly chosen vectors of length  $l_1$  and  $l_m$ . Equation (6) is valid only for the case when  $|\vec{R}_{i+1} - \vec{R}_i| = |\vec{R}_i - \vec{R}_{i-1}|$ . Since in our model of ionic surfactants  $|\vec{R}_3 - \vec{R}_2| \neq |\vec{R}_2 - \vec{R}_1|$ , equation (6) needs to be modified for the particle which has unequal bond distances on either side (particle 2 in our case). For such a particle in a given chain (denoted as the  $i$ th particle) if we choose the origin at particle  $i - 1$ , the generalized kink-jump algorithm becomes  $\theta \rightarrow -\theta$ . Here

$$\theta = \cos^{-1} \frac{\vec{d}_{i+1,i-1} \cdot \vec{d}_{i,i-1}}{|\vec{d}_{i+1,i-1}| |\vec{d}_{i,i-1}|} \quad (8)$$

and  $\vec{d}_{i,j}$  is the vector along the bond from the  $i$ th to the  $j$ th monomer. For fixed bond lengths the above equation reduces to equation (6) without requiring going through the more expensive computation of the angle. We have incorporated these *generalized kink-jump* moves for the tail particles next to the ionic head. The factors pertaining to an efficient algorithm, e.g. a link-list and calculation of the energy difference between before and after a move, are the same as described in I. In the following section we discuss the simulation results.

### 3. Results

We first discuss some details of the simulation. We have carried out simulation for  $N_m = 7$  and 10 and for several values of  $N_c$  between 200 and 500. All of the results reported here are carried out at  $T = 0.5$  and in a simulation box of length  $100\sigma_H$ . Typically we wait for 500 000 MC steps (defined earlier) to allow micelles to form and equilibrate. A further  $10^6$  MC steps are used to calculate the cluster distribution and structure factor at every 1000th MC step.

#### 3.1. Ionic micelles

First, we show the results for aggregation of ionic surfactants only. Figure 1 shows typical snapshots of surfactant aggregation for  $N_m = 7$  and  $R_b = 0.2$  as a function of  $N_c$  at the end of 500 000 MC steps. The corresponding cluster distributions are shown in figure 2. It is noticeable that with increasing concentration, the occurrence of larger clusters becomes more probable and the cluster distribution function develops a tail. At even larger concentrations (figure 1 (bottom right)) the micelles no longer retain their spherical (circular in 2D) shapes. They become elongated along one direction instead. This is consistent with the known experimental phase diagram for surfactants which shows that cylindrical micelles occur at larger concentrations [7]. With increasing cluster sizes, it becomes increasingly difficult to equilibrate the system, and finite-size effects become severe as well [16]. We thus refrain from showing the cluster size distribution for this concentration<sup>5</sup>.

<sup>5</sup> To equilibrate the system for larger concentrations, reptation and kink-jumps may not be very efficient. We believe that cluster–cluster aggregation moves will equilibrate the system much faster. We will report numerical results for higher surfactant densities using these moves in a later publication.

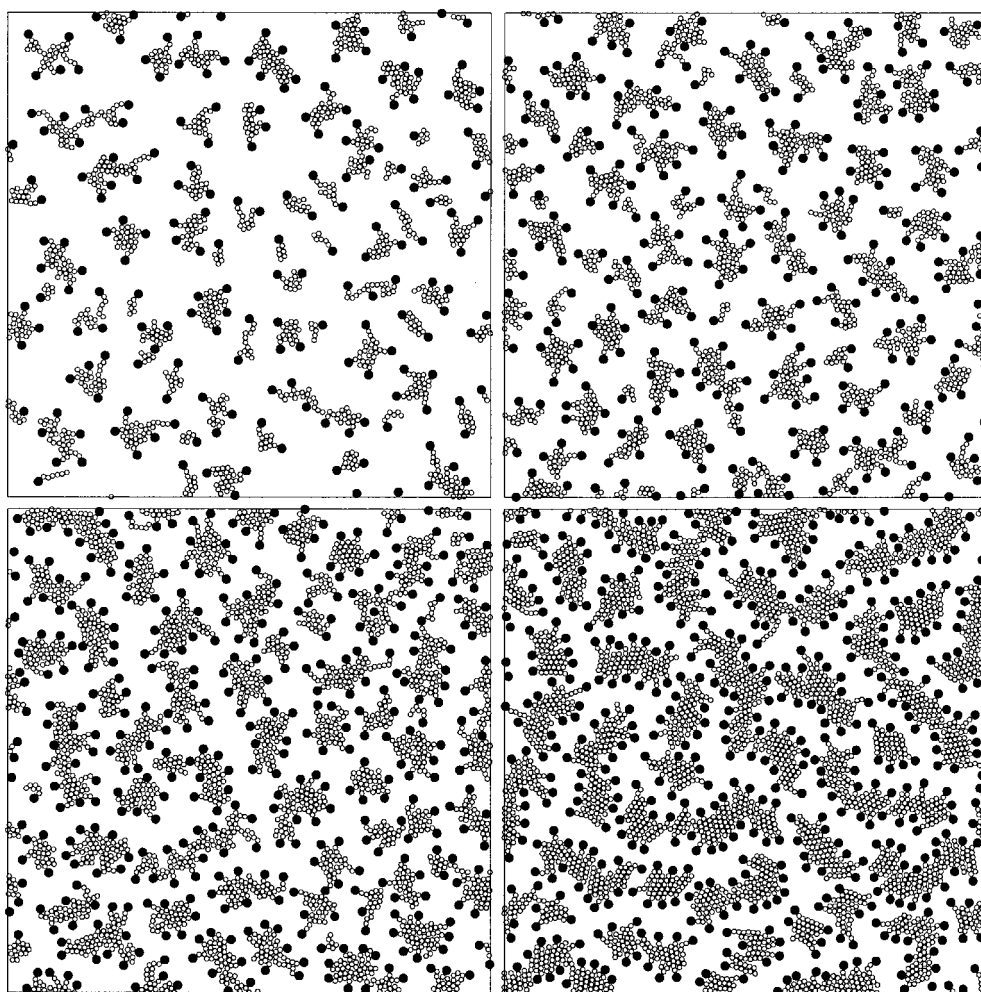


**Figure 1.** Snapshots of micellar aggregation for ionic surfactants for  $T = 0.5$ ,  $R_b = 0.2$ ,  $N_m = 7$ , and for  $N_c = 200$  (top left),  $N_c = 300$  (top right),  $N_c = 400$  (bottom left),  $N_c = 500$  (bottom right), at the end of 500 000 MC time steps. Open and closed circles represent the tail and head particles respectively.

The simulation results for ionic surfactants obtained from these off-lattice MC studies without explicit incorporation of the solvent degrees of freedom contain qualitatively similar features to those found in earlier lattice MC calculations and MD studies of neutral surfactants which took into account the solvent degrees of freedom explicitly [17–23]. Longer-range SC interactions do not alter the qualitative features of the surfactant aggregation. The cluster distribution of ionic micelles is very similar to what one obtains with neutral micelles. However, the calculated structure factor of the centres of mass of the ionic micelles shows an additional peak as shown in figures 2(d)–2(f) which is absent for neutral micelles [14]. A SC interaction among the surfactant heads introduces a repulsive interaction among the micelles which makes them more ordered. We have checked that the  $k$ -value corresponding to the peak of the structure factor for each concentration does indeed correspond to the average distance between any two neighbouring micelles. Our simulation results clearly demonstrate how one can study

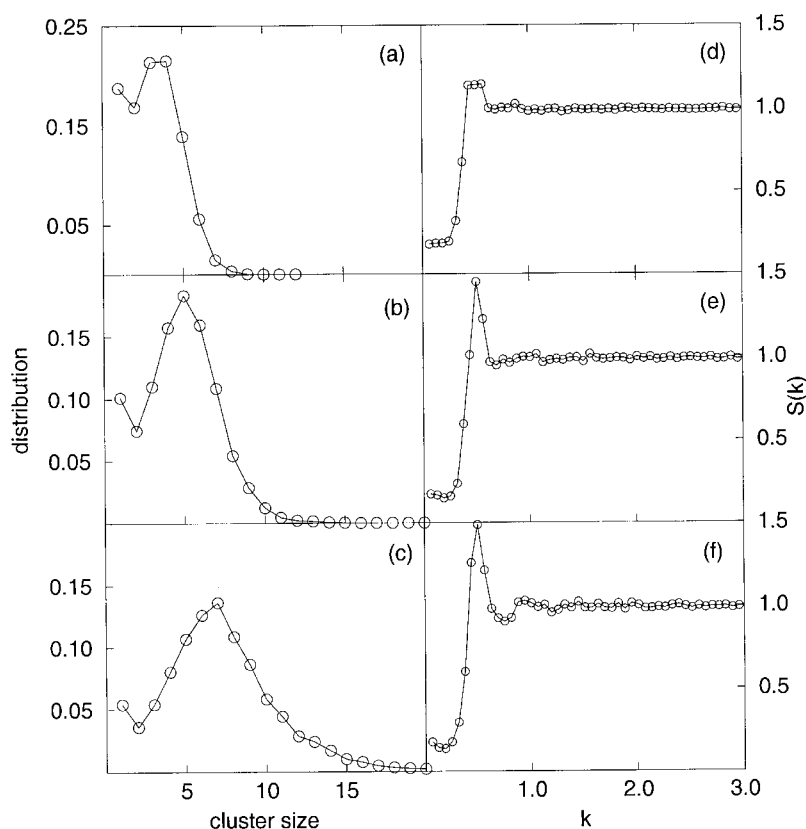


**Figure 2.** Time-averaged cluster distributions and structure factors for ionic surfactants corresponding to the first three snapshots shown in figure 1. The time average is taken every 1000 steps over the last 500 000 MC steps. The peaks in the structure factor  $S(k)$  correspond to the averaged separation among the micelles.

properties of ionic surfactants in a simple model by introducing a phenomenological SC interaction among the surfactant heads. Ordering of ionic micelles is a well known experimental result. However, the earlier numerical studies [17–23], except ours [14], were all restricted to neutral micelles. This is the first detailed study of the aggregation properties of ionic surfactants where *intermicellar interactions* have also been taken into account.

Figure 3 shows the effect of the bending parameter  $R_b$  for surfactants of chain length  $N_m = 10$ . The corresponding cluster distributions and structure factors for the micelles are shown in figure 4. For rigid surfactants (large values of the bending parameter  $R_b$ ) there is a tendency to form larger clusters. We found similar features in our studies of neutral micelles. The shapes of the micelles change from circular to linear with increase in bending rigidity. In the linear structure the surfactants line up side by side. We have argued in I that for linear structures, which are essentially one dimensional, the average energy per surfactant shows a rather weak dependence on the aggregation number. This results in an increased polydispersity in the micellar size distribution [14]. A similar situation also occurs for charged surfactants. The only difference is that the charged head groups alternate from one side to the other to reduce the Coulomb repulsion energy. It is worth noting that since the simulation method eliminates solvent degrees of freedom, it has been possible to obtain results where many

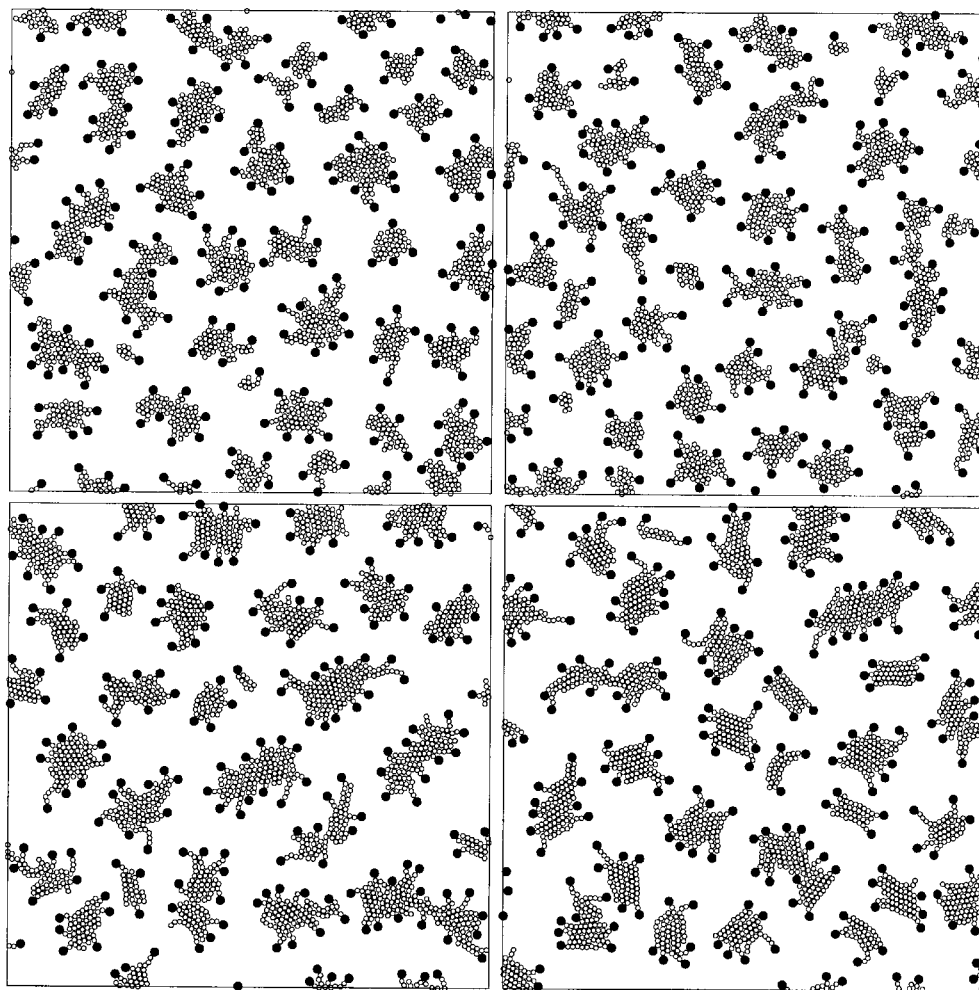


**Figure 3.** Snapshots of micellar aggregation for ionic surfactants for  $T = 0.5$ ,  $N_m = 10$ , and for  $N_c = 210$  as a function of the bending parameter  $R_b$ :  $R_b = 0.0$  (top left),  $R_b = 0.2$  (top right),  $R_b = 0.4$  (bottom left),  $R_b = 0.6$  (bottom right), at the end of 500 000 MC time steps. The symbols have the same meaning as in figure 1.

micelles are present and therefore quantitative statements can be made about intermicellar effects on the basis of the structure factor data. Previous studies with large numbers of micelles were restricted to lattice models of neutral surfactants only [18].

### 3.2. Ionic surfactants and host particles

We now present the simulation results for surfactant self-assembly with other host particles. We have mentioned in the introduction that these studies are relevant to the experiments on fabricating nanostructures and mesostructures through surfactant-directed-templating routes. Dissolved solutes that interact strongly with the surfactants have a large effect on the structures and properties of surfactants in solution. Host particles with purely repulsive (excluded-volume) interaction with the surfactants decrease the effective available volume and hence



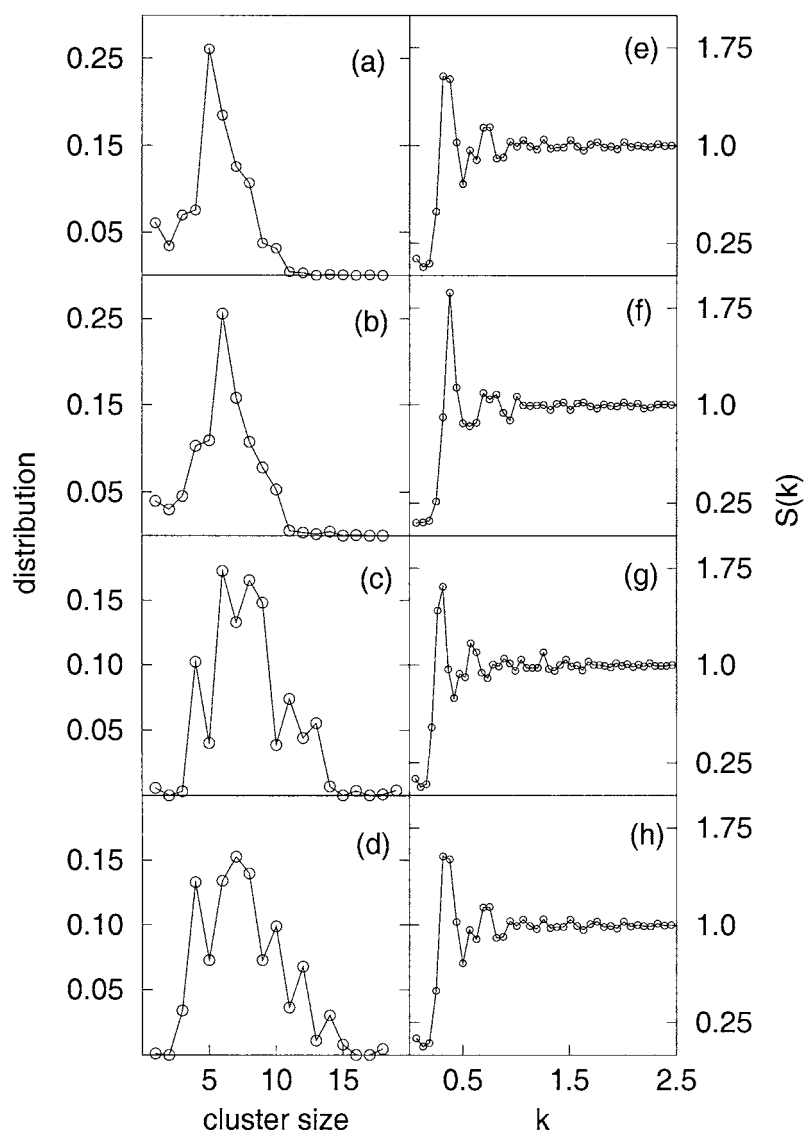


**Figure 4.** Time-averaged cluster distributions (panels (a), (b), (c), (d)), and structure factors (panels (e), (f), (g), (h)) for ionic surfactants for the snapshots shown in figure 3. The time average is taken every 1000 steps over the last 500 000 MC steps. The first peak in each  $S(k)$  corresponds to the average separation among the micelles.

change the effective concentration and size distribution of micelles. With an attractive interaction, the host particle can affect the final structures significantly.

The experiments that are carried out are broadly of two types. In the first and traditional approach one considers a pre-assembled micellar configuration as a structure-directing element. Further pattern formation by the host particle mimics this pre-formed structure. This is the idea behind the so-called *biomimetic* approach. In the second procedure the synthesis process begins from a soup of surfactants and the host particles. In our simulation we have considered two different initial conditions. In the first case we study the pattern formation by adding host

particles to pre-formed micellar structures of surfactants. In the second case we take the initial configuration to be a completely random distribution of surfactants and the host particles.

- (i) *Host particles added to pre-formed micelles.* In this case we start with an initial arrangement of surfactants as shown in figure 3 (top left) with a random distribution of host particles in the rest of the available space. The host particles are first allowed to distribute uniformly by turning on a purely repulsive interaction among themselves after which the actual interactions as described in table 1 are turned on. We then allow MC moves for both the surfactants and the host particles and look for the final configuration for the surfactant–host composite. Typical snapshots are shown in figure 5 for  $N_p = 1000$ ,  $\epsilon_{pp} = 0.5$ ,  $\epsilon_{hp} = 1.0$ . The only parameter which is different for the top and bottom pictures is the particle size  $\sigma_{pp}$ , which is chosen as  $\sigma_{pp} = \sigma_{tt}$  (top) and  $\sigma_{pp} = 2\sigma_{tt}$  (bottom). We have found that the ordering of host particles shown in figure 5 can be qualitatively explained solely in terms of the dimensionless density parameter  $\bar{\rho}_p = \rho_p \sigma_{pp}^2$ , where  $\rho_p$  is the effective density of the host particles (defined below). We have carried out simulations for several combinations of  $N_p$  and  $\sigma_{pp}$  (summarized in table 2) to study how the dimensionless density  $\bar{\rho}_p$  affects the final surfactant–host composite structure. Since the qualitative features are contained in figure 5, we discuss the results in terms of these two parts (figures 5(a) and 5(b)) only.

**Table 2.**

Surfactant–host systems	$\sigma_{pp}$	$N_h$
Case I	$\sigma_{tt}$	1000
Case II	$2\sigma_{tt}$	1000
Case III	$\sigma_{tt}$	2000
Case IV	$\sqrt{2}\sigma_{tt}$	2000
Case V	$\sigma_{tt}$	4000

A comparison of the two snapshots in figure 5 immediately reveals that the host particles exhibit more ordering for the bigger particles, although in the two cases the number densities of the particles are the same. The effects of the host particles on the micelles are noticeable but small. The possible origin of this additional ordering for the bigger particles can be qualitatively explained in terms of the known results of the liquid–vapour coexistence diagram of a 2D LJ fluid [27]. The energies of the pre-formed micelles are almost an order of magnitude larger than the energy of interaction of host particles either with micelles or among themselves. Therefore, to a first approximation, one can think of these micelles as *quenched disorder*. The nature of ordering of host particles can then be predicted from the known phase diagram of the 2D LJ fluid [27] by making a simple calculation of the available volume of each species. Let us define the available area of a surfactant using its LJ parameters. A rough estimate of the total surfactant area is

$$A_{surf} = N_c \left[ (N_m - 1) \pi \left( \frac{\sigma_{tt}}{2} \right)^2 + \pi \left( \frac{\sigma_{hh}}{2} \right)^2 \right].$$

The area of the simulation box is  $A_{total} = 10\,000 \sigma_{tt}^2$ . Therefore, the available area for the host particles  $A_{avail} = A_{total} - A_{surf}$ . For the simulation considered here,  $N_c = 210$  and  $N_m = 10$ , which gives  $A_{surf} = 2144 \sigma_{tt}^2$ , and the effective density of the host particles (in both figure 5(a) and 5(b))  $\rho_p = N_p / A_{avail} = 0.127$ . For  $\sigma_{pp} = \sigma_{tt}$  (figure 5(a)) and  $\sigma_{pp} = 2\sigma_{tt}$  (figure 5(b)) this yields  $\bar{\rho}_p = 0.127$  and 0.509 respectively.

For a 2D LJ fluid, the critical temperature and density is given by 0.522 and 0.344 and the coexistence curve has also been calculated independently in several studies [27].

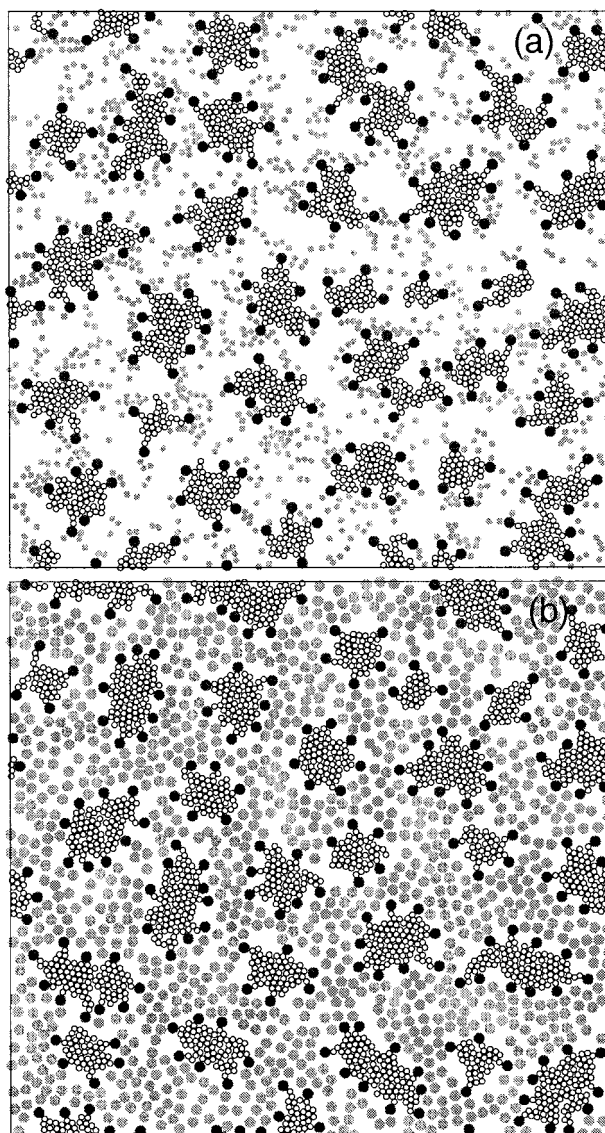


**Figure 5.** Surfactant–host self-assembly for  $N_p = 1000$ ,  $\epsilon_{pp} = 0.5$ ,  $\epsilon_{hp} = 1.0$ . (a)  $\sigma_{pp} = \sigma_{tt}$ , (b)  $\sigma_{pp} = 2\sigma_{tt}$ . Open black, filled black, and filled grey circles refer to the tail, head, and host particles respectively.

We now see that for the first case, considered in figure 5(a) for our simulation temperature  $T = 0.5$ , the value of  $\rho = 0.127$  is too small for any liquid-like characteristics to be exhibited. The second case, shown in figure 5(b), in contrast, corresponds to a higher value of the density and hence the host particles exhibit more liquid-like short-range correlation. We have carried out simulations for three more different cases for the host particles, all of which support this interpretation. Since the results are qualitatively similar to the cases I ( $\bar{\rho}_p = 0.127$ ) and II ( $\bar{\rho}_p = 0.509$ ) considered above, we do not show any snapshots but just state the results. Cases III and IV correspond to  $N_p = 2000$ ,  $\sigma_{pp} = \sigma_{tt}$

and  $N_p = 2000$ ,  $\sigma_{pp} = \sqrt{2}\sigma_{tt}$  respectively.  $\bar{\rho}_p$  for these cases corresponds to 0.254 and 0.509 respectively. According to our interpretation, the local ordering for case III will be intermediate between those for cases I and II. Since  $\bar{\rho}_p$  for case IV is the same as that for case II, we expect similar ordering. Case V ( $N_p = 4000$ ,  $\sigma_{pp} = \sigma_{tt}$ ) again corresponds to  $\bar{\rho}_p = 0.509$ . Consistent with the above argument, we do indeed see local ordering for cases IV and V but not for case III.

In order to be able to make a more quantitative statement regarding the local order of the host particles around micelles, we have calculated the structure factors for the host particles only, leaving aside the micelles. They are shown in figure 6 (solid line). We show the structure factors for the first four cases. The first sharp peak around  $k \sim 0.33$  is present in all cases. This corresponds to the average diameter of the micelles, by which the host particles are separated. This is the largest length scale for the host particles. For cases II and IV we also notice additional peaks for larger values of  $k$ . These peaks correspond to the more ordered local structure of the host particles. For case II the secondary peaks occur for  $k \sim 3.1$  and  $6.2$  and correspond to a length  $\sim 2^{1/6}\sigma_{pp} = 2^{1/6}(2\sigma_{tt})$ . Likewise, the secondary peaks for case IV occurring at  $k \sim 4.3$  and  $8.6$  correspond to a length  $\sim 2^{1/6}\sigma_{pp} = 2^{1/6}(\sqrt{2}\sigma_{tt})$ . The ratio of the  $k$ -values  $3.1/4.3 \simeq 1/\sqrt{2}$  is inversely proportional to the LJ diameters of the host particles. This proves beyond any doubt that the secondary peaks correspond to the local ordering of the host particles. For case V also we have checked that a peak occurs for the  $k$ -value corresponding to a length  $\sim \sigma_{pp} = \sigma_{tt}$ . An analogous scenario is expected to arise in three dimensions and naturally could be verified experimentally.

- (ii) *Host particles added directly to surfactants.* For our second approach to micelle formation in the presence of host particles we have carried out simulations for an identical set of parameters (to that in (i) above), but starting with a completely random configuration of surfactants and host particles. In spite of the two initial configurations being radically different, we find that the final structures are roughly the same<sup>6</sup>. The structure factors shown in figure 6 for these sets of runs (dotted lines) are almost indistinguishable from the first set (solid lines). One might wonder what the implications are of carrying out the simulation for the second case, as the cases are expected to yield the same results in a typical MC calculation provided that the final structure is an equilibrium configuration. *A priori*, there is no reason to believe that the final complex structures seen in our simulations are the equilibrium structures. The fact that we see nearly the same structures starting from completely different points in phase space clearly indicates that we are indeed observing true equilibrium structures, rather than some metastable ones. Also it suggests that the barriers from one structure to another are not that high. Otherwise in the second case we might have become trapped in a completely different (metastable) structure.

We find that in the presence of host particles, the sizes and distributions of micelles are hardly affected. This is because the energy associated with the surfactant–host interaction parameters are small compared to the average total energy of a micelle. In addition we have chosen a repulsive interaction between the host particles and the tails of the surfactants. As a result, the likelihood of host particles getting trapped inside the micelles and affecting their structure is very small. On the contrary, the arrangements of the host particles are dictated by the pristine micelles. The concept of biomimetic approach is useful in this case as the pre-formed micelles can act as templates or structure-directing elements for further pattern formation by the host particles with an appropriate value of  $\bar{\rho}_p$ .

<sup>6</sup> We have monitored the energy as a function of MC steps to check how the systems approach equilibrium. We find that once the equilibrium is achieved, the energies of the systems for two different sets of initial conditions are the same within the error bar.

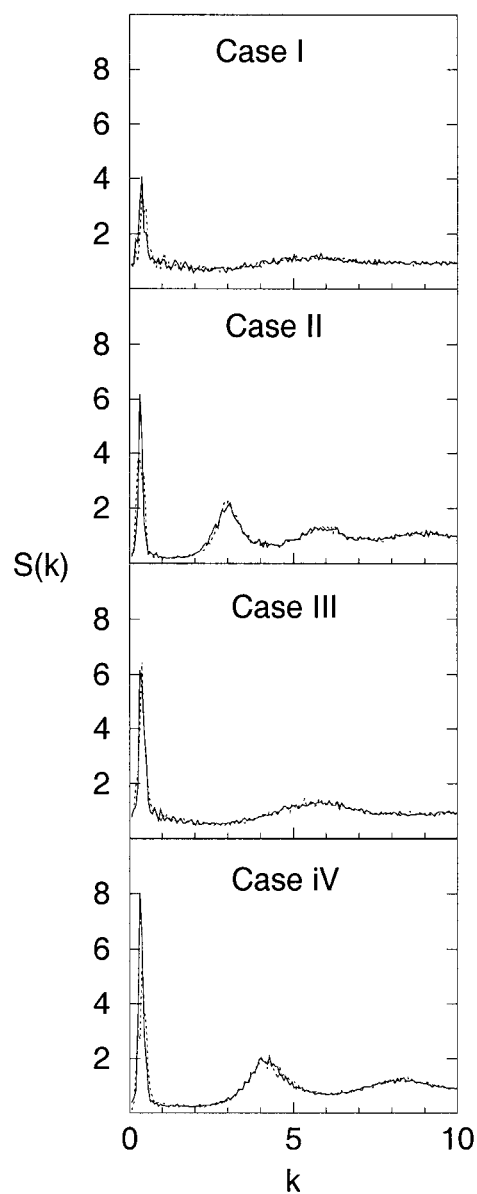


**Figure 6.** Comparison of time-averaged structure factors for the host particles for the four cases mentioned in the text. The solid and dashed lines correspond to surfactant–host self-assembly along pathways 1 and 2 respectively. The structure factors shown in this figure correspond to  $\epsilon_{pp} = 0.5$  and  $\epsilon_{hp} = 1.0$  respectively.

For larger values of the surfactant–host interactions the micellar arrangements cannot be sustained as templates. In this case, even if we start with pre-formed micelles, depending on the detailed nature of the host–head and host–tail interactions the host particles will break micelles into pieces either by getting embedded inside them or by fusing micelles decorated with host particles. In either case the surfactant–host system will evolve into a completely new structure. This is where the standard concept of biomimetic approach

will break down and a more general concept of cooperative self-assembly needs to be invoked. We are looking at these regimes in more detail. Indeed our preliminary results show that if we choose  $\epsilon_{pp} = \epsilon_{hp} = 1$ , leaving all other parameters the same as above, we obtain structures in which micelles are present but with shapes and sizes that are very different from those at the start. In this case the host particles surrounding one micelle attract other host particles surrounding a different micelle more strongly. The resulting fusion of two micelles changes the shape of the pristine micelles.

#### 4. Summary

We have carried out off-lattice MC simulation on ionic surfactants using a very simple model that nonetheless incorporates most of the important physics governing the self-assembly. The solvent degrees of freedom have been eliminated in our model, which helped us to carry out simulations for a large number of surfactants with wide ranges of parameters. In order to study intermicellar correlations, one needs a large number of micelles to form. This was possible with this simulation scheme. Earlier we had used this method to study neutral micelles with LJ potential and bond-bending energies<sup>7</sup>. Here we find that by adding a SC interaction among the surfactant heads to the model of neutral surfactants with LJ and bond-bending potentials, it is possible to reproduce the characteristic structural features of ionic micelles. In this 2D model we demonstrate that ionic surfactants produce micelles which exhibit structural ordering analogous to the hexagonal ordering of cylindrical micelles in 3D. It is worthwhile mentioning that the screening parameters are to be interpreted as adjustable parameters using which one can conveniently interpolate from neutral to ionic micelles.

Having demonstrated the aggregation properties of ionic surfactants alone, we then extended our studies of surfactant aggregation in the presence of other host particles. This was motivated by experiments on preparing mesostructures where surfactants play an active role. We take a simplified approach where we add additional host particles to the ionic surfactants and ask how the final structure is affected by the sizes, interaction strengths, and concentrations of the host particles. Our simulation for several densities of host particles reveals an interesting feature. We find that the structure factor of the host particles exhibits additional local ordering which can be described by the dimensionless density parameter  $\bar{\rho}_p$ . It is evident from these studies that not only the densities of the particles but also their sizes have to be correctly tuned to get mesostructures through surfactant-induced templating. We argued that a simple but more physical picture emerges when micelles are looked at as a source of quenched disorder for the motion of host particles. The ordering of the host particles is then mapped onto the model of a 2D LJ fluid. We find that in order to have an ordered structure of the host particles around micelles, the dimensionless density has to be sufficiently large that it corresponds to a liquid-rich phase in the liquid–vapour coexistence region. This liquid-like property shows up as peaks in the structure factor for large  $k$ -values.

<sup>7</sup> We are grateful to a referee for pointing out the work by Wenzel *et al* [28] where it has been demonstrated that a model for amphiphiles with Ising-like site and bond variables exhibits a critical micelle concentration (CMC) and a closed-loop coexistence curve as seen in experiments [7]. The amphiphiles in this model do not have a structure. That lattice amphiphiles with structures exhibit a CMC has been demonstrated by others and by us in a previous paper [29] in which we have also reported the temperature dependence of the CMC. We have also checked that the lattice counterpart of the off-lattice model used here (without the solvent degrees of freedom) has a CMC with similar temperature dependence [30] as reported in our previous work [29]. However, to the best of our knowledge, none of the models of amphiphilic aggregation explicitly incorporating the structure of the individual amphiphiles have addressed this issue of closed-loop coexistence. Following the referee's comment, we are very interested in addressing this issue.

Finally, as we have adopted a MC approach here, no comparison can be made as regards the actual time that is required for the system to reach the same state from different initial conditions. It would be worthwhile to carry out MD simulations to address such issues, which may be relevant for the synthesis of mesoporous sieves. An extension of these calculations to three dimensions is equally important. We are currently looking into some of these aspects, which we will report on in a separate publication [30].

## Acknowledgments

It is our pleasure to thank Professor Kurt Binder, Professor Amit Chakrabarti, Professor Andrey Milchev and Professor T J Pinnavaia for discussions. This work was supported by National Science Foundation Grant number CHE-99-03706. Partial computer support through Michigan State University is gratefully acknowledged.

## References

- [1] Kresge C T, Leonowicz M E, Roth W J, Vertuli J C and Beck J S 1992 *Nature* **359** 710  
Davis M E 1994 *Proc. MRS Spring Meeting on Better Ceramics through Chemistry VI* (Pittsburgh, PA: Materials Research Society)
- [2] Huo Q, Margolese D I, Ciesla U, Demuth D G, Feng P, Gier T E, Sieger P, Firouzi A, Chmelka B F, Schuth F and Stucky G D 1994 *Chem. Mater.* **6** 1176  
Huo Q, Margolese D I, Ciesla U, Feng P, Gier T E, Demuth D G, Sieger P, Leon R, Petroff P M, Schuth F and Stucky G D 1994 *Nature* **368** 317  
Monnier A, Schuth F, Huo Q, Kumar D, Margolese D, Maxwell R S, Stucky G D, Krishnamurty M, Petroff P, Firouzi A, Janicke M and Chmelka B M 1993 *Science* **261** 1299
- [3] Beck J S, Vertuli J C, Roth W J, Leonowicz M E, Kresge C T, Schmitt K D, Chu C T-W, Olson D H, Sheppard E W, McCullen S B, Higgins J B and Schlenker J L 1992 *J. Am. Chem. Soc.* **114** 10 834
- [4] Tanev P T and Pinnavaia T J 1995 *Science* **267** 865  
Tanev P T and Pinnavaia T J 1996 *Chem. Mater.* **8** 2068  
Tanev P T and Pinnavaia T J 1995 *Access in Nano-Porous Materials* ed T J Pinnavaia and M F Thorpe (New York: Plenum)  
Attard G S, Glyde J C and Goltner C J 1995 *Nature* **378** 366
- [5] McGrath K M, Dabs D M, Yao N, Aksai I A and Gruner S M 1997 *Science* **277** 552
- [6] For reviews, see  
Mittal K L and Bothorel P (ed) 1985 *Surfactants in Solution* (New York: Plenum)  
Mittal K L and Lindman B (ed) 1984 *Surfactants in Solution* (New York: Plenum)  
and other volumes in this series. See also  
deGiorgio V and Corti M (ed) 1985 *Physics of Amphiphiles: Micelles, Vesicles and Micro-Emulsions* (Amsterdam: North-Holland)
- [7] Laughlin R G 1994 *The Aqueous Phase Behavior of Surfactants* (New York: Academic)
- [8] Yang H, Coombs N, Sokolov I and Ozin G A 1996 *Nature* **381** 589
- [9] Schacht S, Huo Q, Voigt-Martin I G, Stucky G D and Schuth F 1998 *Science* **273** 768
- [10] Mann S 1993 *Nature* **365** 499  
Mann S 1993 *Science* **261** 1286
- [11] Israelachvili J 1985 *Intermolecular and Surface Forces* (New York: Academic)
- [12] Palmer B and Liu J 1996 *Langmuir* **12** 6015
- [13] For a review see  
Gompper G and Schick M 1994 *Phase Transitions and Critical Phenomena* vol 16 (New York: Academic)
- [14] Bhattacharya A, Mahanti S D and Chakrabarti A 1998 *J. Chem. Phys.* **108** 10 281  
Detailed references to previous Monte Carlo and molecular dynamics simulations are given in this paper along with an extended discussion of the method that we have adopted.
- [15] Viduna D, Milchev A and Binder K 1998 *Macromol. Theory Simul.* **7** 649  
Milchev A, Bhattacharya A and Binder K 2001 *Macromolecules* submitted
- [16] Nelson P H, Rutledge G C and Hatton T A 1997 *J. Chem. Phys.* **107** 10 777
- [17] Egberts E and Berendsen H J C 1988 *J. Chem. Phys.* **89** 3715

- [18] Desplat J-C and Care C M 1994 *Mol. Phys.* **87** 441 and references therein
- [19] Mackie A D, Panagiotopoulos A Z and Szleifer I 1997 *Langmuir* **13** 5022  
Wijmans C J and Linse P 1995 *Langmuir* **11** 3748
- [20] Rector D R, van Swol F and Henderson J R 1994 *Mol. Phys.* **82** 1009
- [21] Smit B, Esselink K, Hilbers P A, van Os N M, Rupert L A M and Szleifer I 1993 *Langmuir* **9** 9
- [22] Smit B, Hilbers P A, Esselink K, Rupert L A M and van Os N M 1991 *J. Chem. Phys.* **95** 6361
- [23] Palmer B and Liu J 1996 *Langmuir* **12** 746
- [24] Wall F T and Mandel F 1975 *J. Chem. Phys.* **63** 4592
- [25] Verdier P H and Stockmayer W H 1962 *J. Chem. Phys.* **36** 227
- [26] Grest G S, Dunweg B and Kremer K 1989 *Comput. Phys. Commun.* **55** 269
- [27] Frenkel D and Smit B 1991 *J. Chem. Phys.* **94** 5663
- [28] Wenzel W, Ebner C, Jayaprakash C and Pandit R 1989 *J. Phys.: Condens. Matter* **1** 4245
- [29] Bhattacharya A and Mahanti S D 2000 *J. Phys.: Condens. Matter* **12** 6141  
See also references cited therein for other relevant work on lattice amphiphiles.
- [30] Bhattacharya A and Mahanti S D 2001 *J. Phys.: Condens. Matter* to be submitted